

2020

Sindbis virus infects specific gut cells for replication and dissemination from the posterior midgut of mosquitoes

Yani P. Ahearn

University of North Florida, n00879741@unf.edu

Follow this and additional works at: <https://digitalcommons.unf.edu/etd>



Part of the [Laboratory and Basic Science Research Commons](#)

Suggested Citation

Ahearn, Yani P., "Sindbis virus infects specific gut cells for replication and dissemination from the posterior midgut of mosquitoes" (2020). *UNF Graduate Theses and Dissertations*. 959.
<https://digitalcommons.unf.edu/etd/959>

This Master's Thesis is brought to you for free and open access by the Student Scholarship at UNF Digital Commons. It has been accepted for inclusion in UNF Graduate Theses and Dissertations by an authorized administrator of UNF Digital Commons. For more information, please contact [Digital Projects](#).

© 2020 All Rights Reserved

Sindbis virus infects specific gut cells for replication and dissemination from the posterior midgut of mosquitoes

By

Yani Ahearn

A thesis submitted to the Department of Biology
in partial fulfillment of the requirements
for the degree of Master of Science in Biology
UNIVERSITY OF NORTH FLORIDA
COLLEGE OF ARTS AND SCIENCES
April 2020

Acknowledgement

I would like to first thank my thesis adviser, Dr. Bowers, for her expertise and constant encouragement during my pursuit of personal growth and scientific journey in the last three years. I have known you since I came to this country 10 years ago, and you have been one of the few people who has witnessed how much I've struggled all these years and came to be the person I am today. You have always been there as my mentor whenever I needed your advice, whether it was personal or academic, and I know I can always come to you when I need support. I would also like to thank my committee members, Dr. Smith and Dr. Waddell, for your support during a time of global crisis unlike any other that we have experienced before. Thank you both for making it possible for me to defend my thesis in a definitely nontraditional way to say the least.

Mom and dad, thank you for always being there for me through the thick and thin, and I know you will always support me no matter what it is that I am going through. Thank you both for giving me a loving family and trying your best to pave a path for my life here in this country. We may not always agree on everything, maybe more so lately, but I know we will always be family and I will always have a place called home wherever I am. Thank you, mom, for your unconditional love, and dad, for your guidance and support through all these years. I would not be the person I am today without the contributions and sacrifices you both have had to make.

Thank you, Tim, you are my rock and the best cheerleader one can ever hope for. You've always believed in me, even in times I had doubts about myself, and, for some strange reason, you are always so confident that I am up to face my challenges. I am grateful for the time we've had together, and I look forward to having many more years together being our silly selves.

Lastly, but certainly not least, thank you Terese and Joe, for providing food and opening your home to me during a challenging time. Thank you both for your support and making me feel like at home. You both are always so positive and thoughtful, and I am really happy to be part of your family.

P.S. Cinnamon, thank you for being the best companion any human can hope for.

Table of Contents

Title Page	i
Certificate of Approval	ii
Acknowledgements	iii
Table of Contents	iv
List of Figures	vi
Tables	v-vi
Abstract	vii
Chapter 1: Introduction	1-8
Chapter 2: Materials and Methods	9-11
Chapter 3: Results	12-26
Chapter 4: Discussion	27-30
References	31-33
Vita	34

List of Figures

Fig. 1 Laser confocal micrograph of persistent non-disseminated SINV infection in *Aedes aegypti* at day 30 p.i.. The posterior midgut (PMG) is comprised of three distinct regions: PMG-frontal (PMG-f), PMG-middle (PMG-m), and PMG-caudal (PMG-c). A single SINV associated GFP infection focus is restricted to the PMG-m and PMG-m regions. Image from Saredy and colleagues (2020).

Fig. 2 *Aedes aegypti* midgut cross section. Morphological evidence of enteroendocrine cells (EC) in the PMG of mosquito. ECs have a conical, flask-like shape and lack basal membrane labyrinth, unlike neighboring digestive cells (DC). MV, microvilli. Image by Jason Saredy.

Fig. 3 Diagrams showing unmodified parental SINV (A) and insertion of TaV 2A-like protease and GFP (B) and genomic structure of capsid autoprotease and *Thosea asigna* virus 2A-like protease sequence. (Sun et al., 2014)

Fig. 4 Plaque assay showing dilutional effect of SINV. Baby hamster kidney-21 cells were infected with SINV-TaV-GFP and the final titer was calculated using plaque counts and known dilution factors.

Fig. 5 Fluorescent confocal image (A) and bright field overlay (B) of multiple SINV-TaV-GFP infection foci in the midgut of *Ae. aegypti* on day 5 p.i. Female mosquitoes were proffered viremic bloodmeal and guts were dissected on day 5 p.i. SINV infection foci are shown as green fluorescent clusters. White arrows indicate width of the midgut (A). HG: hindgut MP: Malpighian tubules. MG: midgut. 100X.

Fig. 6 Distribution of ECs in the mosquito PMG on day 5 p.i. ECs with FMRFamide granules are demonstrated by TX-Red fluorescence and indicated by white arrows in all three images. N: potential neuron. MG: midgut. A. 100X B. 200X. C. 400X

Fig. 7 Confocal fluorescent images of FMRFamide positive ECs (A) and a single GFP focus extending from front to back of the midgut (B & C) and overlay of the GFP infection foci and TX-red fluorescence (D). Midgut of a female *Ae. aegypti* dissected on day 5 p.i. GFP infection foci did not colocalize with FMRFamide-positive ECs. 200X.

Fig. 8 Overlay confocal fluorescent image of FMRFamide positive ECs and a GFP infection foci in the caudal midgut region of a female *Ae. aegypti* dissected on day 7 p.i. with SINV. GFP infection foci did not colocalize with FMRFamide-positive ECs. 200X.

Fig. 9 Overlay confocal analysis of SINV associated GFP (A) and ECs associated TX-Red (B) in PMG infection focus in mosquito-1 at day 7 p.i. A. SINV associated GFP accumulations at the basolateral aspect of the PMG. B. FMRFamide-positive EC on the basal aspect of the PMG region. A & B 200X. C. Overlay of A&B. 200X.

Fig. 10 GFP accumulations and FMRFamide immunoreactivity in PMG of mosquito-2 on day 7 p.i. ECs are indicated with white arrows. A. GFP accumulations, 20X. B. FMRFamide immunoreactive ECs. 200X.

C. Overlay of GFP accumulations and ECs at two distinctive sites, 200X. D. DIC image showing the colocalizations, 200X.

Fig. 11 Confocal analysis of GFP infection foci and ECs in the posterior midgut region of mosquito-3 day 7 p.i. A. Single GFP infection focus. B. FMRFamide positive ECs. C. Confocal microscopy with brightfield overlay showing ECs and the structure of the midgut. D. Overlay of A, B, & C showing GFP accumulations in ECs. 200X.

Fig. 12 Laser confocal micrograph showing distribution of ECs in midgut of a non-bloodfed female mosquito. Immunoreactive ECs are peppered along the entire length of the gut. A. Confocal microscopic image of ECs. B. Brightfield overlay showing overall structure of the gut. Malpighian tubules are present to indicate posterior midgut region. 200X.

Fig. 13 Laser confocal micrograph showing distribution of ECs in midgut of a bloodfed female mosquito on day 5 p.i. Immunoreactive ECs are shown along the entire length of the gut. A. Confocal microscopic image of ECs. 200X B. Confocal image of the same mosquito showing structure of ECs.600X.

Fig. 14 Confocal microscopy of ECs in midgut of day 5 post viremic bloodfed female mosquito. Immunoreactive ECs are observed along the entire length of the gut. A. Confocal microscopic image of ECs. 20x B. Confocal image demonstrating structures of ECs and peristaltic muscle bundles. 400X. C. Confocal image showing individual ECs. 600X.

Fig. 15 Confocal microscopy of ECs in midgut of day 7 post bloodfed female mosquito. A few immunoreactive ECs indicated by white arrows were observed in the basal aspect of the midgut. A. Confocal microscopic image of ECs. 200X. B. Confocal image showing the structure of the midgut. 200X.

Fig. 16 Confocal microscopy of ECs in midgut of day 7 post viremic bloodfed female mosquito. Immunoreactive ECs were observed in the basal aspect of the midgut. A. Confocal microscopic image of ECs. 20X. B. Confocal image showing the structure of the midgut. 200X.

Fig. 17 Comparison of mosquito midguts positive for FMRFamide after bloodfeeding treatments. Female mosquitoes received no bloodmeal (No BM) on day 0, normal bloodmeal (NBM) on day 5 and 7, viremic bloodmeal (VBM) on day 5 and 7.

Fig. 18 Confocal microscopy demonstrating a SINV associated GFP foci in the PMG-c of a female mosquito at day 30 p.i. The earliest SINV-TaV-GFP infection was observed on day 3 (Saredy et al., 2019; in press) and persistent infection was observed until day 30. A. SINV associated GFP foci. B. Overlay of bright field microscopy demonstrating site of the infection foci. 100X.

Fig. 19 Confocal microscopy of SINV-TaV-GFP dissemination in the PMG-f of a female mosquito at day 30 p.i. SINV associated GFP focus is no longer visible at this stage and local dissemination of SINV is demonstrated via the infection of the peristaltic muscles in the AMG. Anti-FMRFamide treatment demonstrates the presence of ECs in red in this region on day 30. 400X.

Fig. 20 Multiple GFP foci midgut region of female mosquito D7 p.i. Female mosquitoes were proffered viremic bloodmeal and midguts were dissected on D7. GFP foci are indicative of the virus infection within the mosquito midgut. 200X.

Table 1. Percent infection of mosquito midguts and distribution of SINV associated GFP foci in midguts at day 7 p.i.

Table 2. FMRFamide labeled ECs in mosquitoes receiving different bloodmeal (BM) treatments on day 5 vs day 7. (NBM: normal bloodmeal; VBM: viremic bloodmeal; N/A: not sampled).

Table 3. Percent infection and distribution of SINV-TaV-GFP foci in mosquito midgut at day 30 p.i. Mosquito infected.

Abstract

Sindbis virus (SINV), a member of the genus Alphavirus, is the prototype virus used to gain insight into other disease-causing Alphaviruses. As a mosquito-borne-virus (arbovirus), SINV transit in adult female mosquitoes includes attachment to the gut lumen and entry into the midgut cells, followed by replication and dissemination into the hemolymph through yet unknown specific mechanisms. Free-mated adult females, aged day 5-7, were fed a viremic bovine blood suspension via blood sausage at a final SINV titer at 10⁷ PFU/ml. Midguts from fully engorged mosquitoes were dissected on day 5 and 7 post-bloodmeal and further examined by immunolabeling using FMRFamide antibody against enteroendocrine cells (EC). The results were investigated via confocal microscopy and distribution of SINV and ECs were documented. Oral infection of mosquitoes with SINV-TaV-eGFP led to GFP expression along the basal aspect of the posterior midgut (PMG) epithelial monolayer as early as day 5 p.i., persistent infection and dissemination of the virus was observed on day 30 p.i. following viremic blood feeding. ECs were observed along the entire length of the midgut with majority of ECs concentrated in the posterior midgut region. Additionally, our results demonstrated that SINV could indeed infect ECs and the accumulations of SINV associated GFP fluorescence coincided with these cells. Here we propose that ECs, positioned along the basal plasma membrane of the PMG, are involved in SINV dissemination pathway. Due to unique roles that ECs have in the exocytosis of secretory granules from the MG, these cells might serve as a gateway for virus entry into the host hemolymph. These findings suggest that midgut ECs are integral to arbovirus infection, dissemination, and availability for transmission.

I. Introduction

Arthropod-borne-viruses (arboviruses), the etiologic agents of vector-borne diseases, are transmitted by hematophagous insects such as mosquitoes, ticks and midges (Chamberlin, 1980; Sick et al., 2019). Altogether these viruses pose a major health burden worldwide (WHO 2020). Since the beginning of the 20th century, disease incidence and associated deaths have been on the rise due to increasing vector habitat range for some vectors associated with global warming. Vector-borne diseases account for more than 17% of all infectious diseases worldwide, and billions of people are either at risk of contracting or suffering from diseases, such as malaria and ZIKA (WHO 2020). The WHO estimates that nearly 400 million people suffer from dengue virus (DENV) infections yearly, and more than 400,000 deaths are caused by malaria every year globally, most of which are children under the age of five (Bhatt et al., 2013). Vector-borne disease incidence is highest in the tropics, subtropical regions, and especially in populations that lack proper means for effective vector control. However, it is worth noting that the possibility of re-introduction of these diseases in other parts of the world still remains a serious concern.

In recent years a rise in emerging vector-borne disease outbreaks in the United States and its territories has posed a serious concern with the Public Health services. Out of an estimate of 65,000 cases of vector-borne diseases reported in 2016, the majority of those are tick-borne, located predominantly throughout the eastern parts of the U.S. (Rosenberg et al., 2018). The pattern of mosquito-borne diseases is highly dispersed in the U.S., where West Nile virus (WNV) is the most commonly transmitted pathogen in the continental U.S. with outbreaks reported in Texas during the years 2004 - 2016 (Rosenberg et al., 2018). DENV, carried by Aedine mosquitoes such as *Aedes albopictus* and *Aedes aegypti*, is the fastest spreading arbovirus disease worldwide. Its vector range has spread from Africa to Asia and North America due to international trade and globalization. Although recent reports of Dengue outbreaks in the U.S. have been confined to its territories, it is worth mentioning that limited autochthonous transmission of DENV has occurred in the state of Florida (FL), Hawaii, and Texas, and local transmissions of Chikungunya virus (CHIKV) and ZIKA virus have been reported in TX and FL (Hall et al., 2016).

Human malaria is a serious and sometimes fatal disease caused by several plasmodium species and is transmitted by Anopheline mosquitoes primarily in the tropics and sub-Saharan Africa, and occasionally in the United States (WHO 2017). Plasmodium falciparum, the most prevalent malaria parasite worldwide, causes the most severe clinical form of malaria and is responsible for 99% documented malaria transmission cases in 2016. An estimate of 216 million cases of malaria in the tropics and sub-Saharan Africa were reported to the WHO, and around 1,700 cases are documented each year in the United States. Despite effective means of malaria prevention and treatments, there was a substantial increase of malaria incidences between 2014 and 2016 in the WHO regions of the Americas and other regions of the world. Vector-borne diseases have become an imminent threat to public health authorities worldwide, and it is crucial that government authorities work closely with the scientific community to develop effective strategies in combating further spread of these etiologic agents and minimizing future economic burden.

Several environmental factors have been contributing to the increased intensity of vector-borne pathogens and the longevity of disease progression including rainfall, temperature, and shelter for vectors (Rosenberg et al 2018). Urbanization, international trade and greater access to transportation have brought humans closer together, and with that, comes a greater risk of infection spread globally. By far climatic change poses the greatest threat to human health through its capabilities of modulating the amount of rainfall, temperature extremes, air quality and sea level rises (WHO 2018). The largest contributor to global warming in the 21st century is anthropogenic emissions of greenhouse gases-- environmental pollution originating from human activity--has been on the rise since the beginning of the Industrial Revolution. The continual escalation in anthropogenic greenhouse gas emissions has directly led to global warming, resulting in long term changes in rainfall, temperature extremes, and climate extremes -- including increased incidences of hurricane events, heatwaves, and flash floods in parts of the world. As a direct consequence there has been a huge upward shift in vector-borne disease incidence worldwide. Arthropods are ectothermic organisms and not surprisingly, approximately $\frac{2}{3}$ of arthropod disease vectors are particularly sensitive to temperature fluctuations. The most essential components to larval survival are water and temperature. Since mosquitoes directly lay their eggs onto the water or in areas that will be flooded with

water, an optimal temperature range for mosquito development is somewhere between 16 to 32 degrees Celsius (Bar-Zeeve 1958). Normal temperature fluctuations in the optimal range tend to have minimal effects on mosquito egg development but later larval instar development increases as temperature decreases until the temperature threshold of 9 degrees Celsius is reached. Warmer temperatures and higher rainfall associated with El Niño events have been shown to increase risk of many infectious diseases worldwide, including malaria and other arbovirus outbreaks in Latin America and Southeast Asia (Hales et al., 1999). The combination of these factors and many others not discussed here have been leading to the inevitable outcome of vector expansion into higher latitudes, simply because the eggs simply cannot tolerate high temperatures in the tropics and equatorial regions, and with that comes a new pattern of disease transmission in regions typically not concerned with arthropod-borne diseases.

Many Alphaviruses are known to be important emerging mosquito-borne pathogens. Several Alphaviruses such as CHIKV, O'nyong nyong, as well as Eastern, Western, and Venezuelan equine encephalitis viruses, are known to cause fatal infections in both humans and lower vertebrates, resulting in large human epidemics (Byrnes and Griffin 1998). Most of these pathogens are zoonoses that have wild animals serving as their natural reservoirs, such as birds and bats; however arthropod vectors have bridged the gap between animals and humans allowing rapid transmission of pathogens, which normally would not occur (WHO 2016). Among the mosquitoes that are the best-known arbovirus-transmitting vectors, *Aedes aegypti*, the Yellow Fever mosquito, is a known vector of Sindbis virus (SINV). These mosquitoes are commonly found in the United States, primary in the eastern part of the country, stretching from the East Coast to the Texas Panhandle (Sperança et al., 2006).

Sindbis virus, first isolated in 1952 from mosquitoes in Sindbis, Egypt, is a member of the genus Alphavirus and family Togaviridae (Taylor et al., 1955). SINV is a zoonotic virus that is commonly distributed across several continents including Eurasia, Africa, Oceania and Australia (Adochief et al., 2016). SINV is normally transmitted among bird species via mosquito vectors and clinical outbreaks in humans mainly occur in South Africa and Northern Europe. Patients infected with SINV often exhibits clinical symptoms of rash, fever, arthritis and myalgia, and the latter two are often disabling for some

patients (Turunen et al., 1998). SINV is a T=4 spherical virus that has a plus sense, single-stranded RNA genome that consists of 11,703 nucleotides, a methylated cap on its 5' end, and a 70-nucleotide long poly—A tail on its 3' end (Strauss et al., 1984). Its genome is housed in an icosahedral capsid consisting of 240 capsid monomers and its host-derived lipid membrane consists of 240 trimeric spikes composed of heterodimers of E1 and E2 glycoproteins, which aid in attachment to host cells (Strauss & Strauss, 1994). SINV genome consists of two open reading frames that code for mRNA which subsequently generates four non-structural proteins and five structural proteins. Once SINV enters host cell in a receptor-mediated manner in clathrin coated vesicles, the translation and the assembly of nucleocapsid occurs in the cytosol, and the completion of the virion assembly occurs at the host cell plasma membrane (Spuul et al., 2011; Jose, Snyder & Kuhn, 2009).

As an arbovirus, SINV migrates in adult mosquitoes includes attachment and entry to the midgut, followed by egress from the midgut, multiplication in various tissues and eventually entry into the salivary glands. The trajectory of virus infection has been proposed to follow midgut, hemolymph, peristaltic muscles, hemocytes, and salivary glands (Bowers et al., 1995; Parikah et al., 2009). In order to establish effective arbovirus infection within a mosquito, the virus must first penetrate the peritrophic matrix formed in the midgut upon imbibing of a viremic blood meal and gain access into the midgut cells for further replication before dissemination into the hemolymph (Okuda et al., 2007). Following the initiation of virus infection within the midgut epithelium, a secondary infection is then followed by replication of the virus throughout the whole mosquito (Hardy et al., 1983).

The mosquito alimentary canal is comprised of a tubular thoracic region and three distinct abdominal regions, the foregut, midgut and hindgut (Clements, 1996). The posterior midgut (PMG) where blood digestion occurs is further divided into three distinct regions and each accounts for approximately a third of the MG: PMG-frontal, PMG-middle, PMG-caudal (Fig. 1; Saredy et al., 2019; in press). The MG is composed of numerous simple columnar digestive cells and scattered enteroendocrine cells (ECs), all surrounded by a basement membrane, nerve fibers, muscle bundles and tracheoles (Brown et al., 1985; Bowers et al., 1995; Romoser et al., 2004). The columnar digestive cells or enterocytes are heavily

decorated by microvilli on the apical aspect. Whereas only the open ECs have apical extension with microvilli, a characteristic that is absent on closed ECs (Brown, et al., 1985). Brown and colleagues (1985) estimated that 500 of these basally, solitarily positioned ECs, each approximately 2-6 um in diameter sometimes possess either apical or basolateral extensions or both, and exist in the midgut region of the mosquito. Dark or clear cytoplasm is observed among these cells and the secretory granules are stored along the basolateral membrane.

Upon blood digestion, these secretory granules are released into the extracellular spaces through first fusing with plasma membranes and ultimately emptying contents via exocytosis (Brown et al., 1985). A variety of neuropeptides are also secreted by ECs in the alimentary canal of the mosquito, including pancreatic polypeptide (36 amino acids in length), and phenylalanine-methionine-arginine-phenylalanine-amide (FMRFamide) (Walsh, 1981). FMRFamide was the first cardioexcitatory peptide identified in mollusks and is distributed exclusively in mosquito PMG region where the blood is deposited (Dockary et al., 1981; Greenberg and Price 1983; Brown et al., 1986). Veenstra and colleagues (1995) have identified several other types of neuropeptides secreted by ECs in the female mosquito midgut. Antisera treatment revealed that FMRFamide is exclusively located in the foregut and the junction of the PMG and hindgut, whereas locustatachykinin is only found at the junction, and allatostatin is distributed in the PMG region (Veenstra,1999).

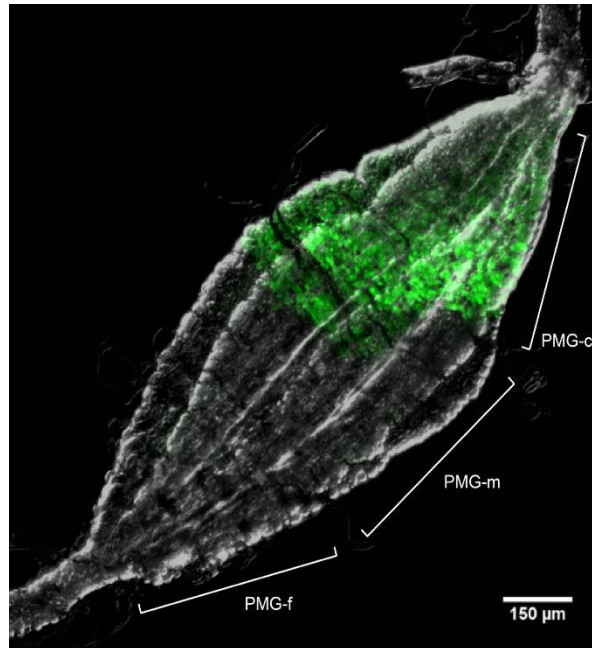


Fig. 1 Confocal microscopy of persistent non-disseminated SINV infection in *Ae. aegypti* at day 30 p.i.. The PMG is comprised of three distinct regions: PMG-frontal (PMG-f), PMG-middle (PMG-m), and PMG-caudal (PMG-c). A single SINV associated GFP infection focus is restricted to the PMG-m and PMG-m regions. Imaged adopted from Saredy and colleagues (2020).

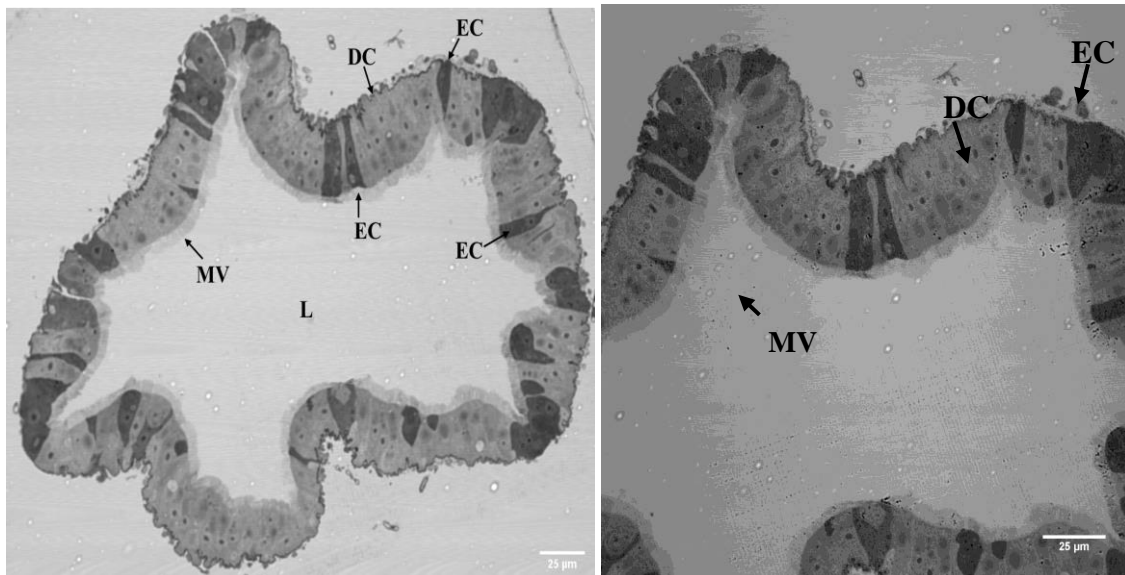


Fig. 2 *Aedes aegypti* midgut cross section. Morphological evidence of enteroendocrine cells (EC) in the PMG of mosquito. ECs have a conical, flask-like shape and lack basal membrane labyrinth, unlike neighboring digestive cells (DC). MV, microvilli. L, lumen. Image by Jason Saredy.

Sindbis is able to infect and replicate in the vector species *Ae. aegypti* upon viremic bloodmeal ingestion and subsequent digestion. Cell surface molecules are important to arbovirus infection and dissemination, however evidence for direct membrane fusion of Sindbis virus has been demonstrated (Vancini et al., 2013). Several cell surface molecules such as laminin receptor, heparan sulfate, and NRAMP have been identified as potential host cell surface receptors for SINV and other Alphaviruses (Rose et al., 2011). As SINV-TaV-GFP replicates in the midgut cells of mosquitoes, it leaves GFP products behind in these cells while continuing to infect other target tissues. These GFP accumulations have been identified possibly in enteric-endocrine cells (Bowers unpublished research). Considering the unique location and functions of these cells, we hypothesize that SINV uses the secretory nature of these cells and the cellular machinery to replicate in great quantity. In this study, the prototype Alphavirus SINV, will serve to gain insight to the biology of other Alphaviruses. The reporter virus used here contains a GFP insert between the capsid protein and E2 (Fig. 3 B) and *Thosea asigna* virus (TaV) 2A-like protease at the 5' end (Fig. 3 C) (Sun et al., 2014; Courtesy of Klimstra lab, University of Pittsburg). GFP products are cleaved upon virus multiplication while the rest of the virus remains intact, thereby allowing us to track the sites of virus infection and dissemination. The primary goal of this study is to examine whether potential roles of ECs in SINV dissemination from the female midgut to other secondary tissues following oral blood feeding.

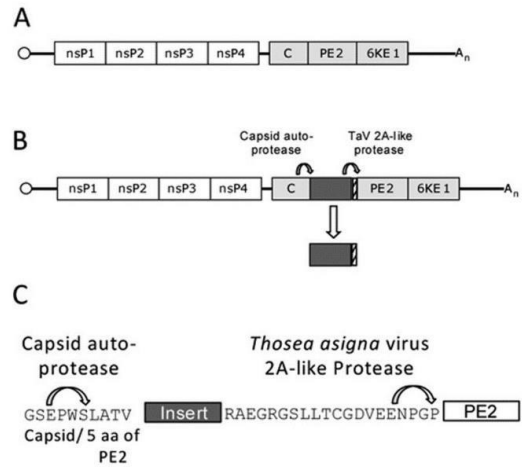


Fig. 3 Diagrams showing unmodified parental SINV (A) and insertion of TaV 2A-like protease and GFP genome (B) and genomic structure of capsid autoprotease and *Thosea asigna* virus 2A-like protease sequence (Sun et al., 2014).

II. Approach and Methods

Hatching and Maintenance of Colony Mosquitoes

Aedes aegypti mosquitoes (USDA, Gainesville, FL) were reared and arbovirus experimentation using whole insects was conducted in the UNF BSL-2 insectary under standard environmental conditions ($25.5 \pm 0.5^\circ\text{C}$, 70-80% humidity, lighting with 30 minutes gradual brightening and 30 minutes of gradual darkening bracketing a 16:8 light/dark photoperiod). Mosquito eggs were hatched in 1.0% nutrient broth (Becton Dickson Microbiology Systems, Sparks, MD). First instar larvae were distributed approximately 300/rearing pan in 1.5 L tap water and fed a 2% liver power suspension (ICN Biochemicals, Cleveland, OH). Following pupation, adults emerged into plastic cages supplied with water-soaked cotton balls for hydration and honey-soaked cellucotton on top of mosquito netting as a carbohydrate source.

Adult female mosquitoes, aged 5-7 days, were supplied with 10ml of warmed defibrinated bovine blood (Colorado Serum Company, Denver, CO) in collagen sausage casings (22mm; The Sausage Maker Inc., Buffalo, NY) as a protein source for egg production. Blood-filled sausage casings were hung vertically (Lyski et al., 2011) in gallon-sized mosquito rearing buckets for an hour at standard conditions. Oviposition cups lined with filter paper were supplied each time after a blood meal and eggs are collected at approximately 3-5 days after feeding. Eggs were stored in a humidity chamber under conditions to ensure proper embryogenesis. Female mosquitoes aged 5-7 days post-emergence (p.e.) were used for the experiment.

Virus and cell culture assays

Sindbis virus TR339, and SINV-TaV-GFP (Sun et al., 2014; gifted by William Klimstra lab) were grown in BHK-21 (baby hamster kidney) cells. These cells were grown in 25 cm² cell flasks at 37C, 5% CO in minimum essential media (MEM) enriched with 5% FBS, 5% TPB, and 20 ul gentamicin. Cells were lifted with 0.25% trypsin and EMEM media refreshed twice a week. A double overlay agarose assay stained with neutral red was used to quantify virus titer by plaque assay (Bowers et al., 1995). Monolayer of BHK

cells were grown to 95% confluency, and SINV/virus growth media (SINV/VGM; 3% fetal bovine serum in PBS) and kept in ice baths before inoculation. Cell media was poured off the cell and SINV/VGM was added to each flask. Virus was allowed to be adsorbed for 1hr with a slow constant rocking on a rocker and periodical rocking by hand. Virus inoculum was pipetted off the monolayer and replaced with 8ml of EMEM. Cells were returned to incubation at 37°C for 24 hrs. Cells were trypsinized off the bottom of cell flasks and centrifuged at 2000X for 2 min at RT. Supernatant was aliquoted and stored at -80°C until needed. Media with 7.5ml of a 1:1 mixture of 2% agarose and 2X MEM media warmed to 42°C. After the agarose mixture was solidified at RT, the cell flasks were incubated at 37°C for two days. Once plaques (clearing of infected cells) were visible, the agarose layer was overlaid with 5ml neutral red mixture consisting of 3ml 3% neutral red and 1% agarose in PBS-D. Final virus titer was calculated to be 2.5×10^7 PFU/ml.

Differential Distribution of Enteroendocrine Cells

Cohorts of mosquitoes were used to examine the differential distribution of ECs in the posterior midguts. Mosquitoes that were not provided a blood meal were dissected on day 0 and the midguts were fixed in 4% paraformaldehyde/PBS (phosphate-buffered saline) and stored overnight at 4 °C until further analysis. Mosquitoes were carbohydrate-starved for 24 hrs prior to receiving either non-viremic or viremic blood meal (1ml SINV in 9ml blood) with a final delivery titer at 2.5×10^6 PFU/ml on day 0. Midguts of replete females were resected on day 5 and 7, followed by fixation and stored overnight at 4 °C. Fixed midguts were rinsed with PBS and incubated with 10% normal goat serum (NGS)/PBS for 1 hr at room temperature. Treated tissues were incubated with anti-FMRFamide primary antibody (Immunostar) at a dilution of 1:100 and followed by gentle rocking overnight at room temperature. Primary antibody was removed, and the tissues were treated with goat-anti-rabbit TX-Red secondary antibody (Invitrogen) for 2 hrs with gentle rocking at room temperature. The specificity of the secondary antibody was ensured by incorporating controls with primary antibody only and secondary antibody only in this experiment. Tissues were analyzed with confocal microscopy to detect the differential distribution of enteroendocrine cells.

Virus infection of mosquitoes

Infectious blood meals were prepared to deliver a final titer of 2.5×10^6 PFU/ml blood. Sindbis virus (SINV TR339-TaV-eGFP) was added to warmed bovine blood contained in a sausage casing and hung in a vertical position inside of each cage for viremic blood-feeding (Lyski et al., 2011). Female mosquitoes were carbohydrate-starved for 24 hours prior to blood-feeding. Females replete with blood were gently moved into labeled cages for incubation at standard insectary conditions as previously described (Bowers et al., 1995). Midguts were resected on days 5 and 7 and positively infected guts with GFP foci were photographed.

Immunofluorescent labeling of mosquito tissues

Mosquitoes were proffered a viremic blood meal with a final titer of 2.5×10^6 PFU/ml SINV-TaV-GFP and engorged females were incubated 5 or 7 days prior to dissection. Midguts were harvested from mosquitoes while viewed through a dissection microscope (Leica Microsystems). Once the midgut was removed, it was transferred into a glass-bottom cell culture dish (Greiner Bio-One) and incubated in 4% paraformaldehyde/PBS for 10 min at RT. The infection foci were captured with a confocal microscope and analyzed using ImageJ. Positively infected guts with visible GFP foci were treated with a blocking agent consisted of 10% normal goat serum (NGS)/PBS for an hour at RT. Immunolabeling was performed using the methods described above. Distribution of FMRFamide was captured on an Olympus FluoView confocal microscope and analyzed with Fiji ImageJ program.

III. Results

Virus amplification in mammalian cell line and quantification using double overlay plaque assay

Monolayers of BHK-21 were grown to 95% confluency prior to virus expression and amplification. Tenfold serial dilutions of virus growth media were prepared for each flask, and the virus was adsorbed for 1 hr at RT on a gentle rocker. Inoculum was discarded and replaced with 2% agarose in PBS. Cell flasks were returned to 37°C and checked every 12 hrs for cytopathic effects, or cell death. Virus plaques were visualized by staining the cells with a neutral red dye that is only taken up by healthy, living cells. Virus expression in BHK cells were imaged during the incubation with the virus. The infecting SINV induced apparent cytopathic effects in the BHK cells lacked GFP fluorescence in all but the negative control flask 24 hrs p.i. (Fig. 4 A). The intensity of GFP fluorescence corresponded to cell density in a dilutional manner in flasks B, C, and D, with the highest density of cells and fluorescence observed in flask B and the lowest in flask D (Fig. 4). Upon viral infection and multiplication, cells infected with SINV displayed visible structural changes including the rounding of cells, lysis of the cells, and eventually cell death. Virus plaques were used to determine the virus titer which was 2.3×10^7 PFU/mL.

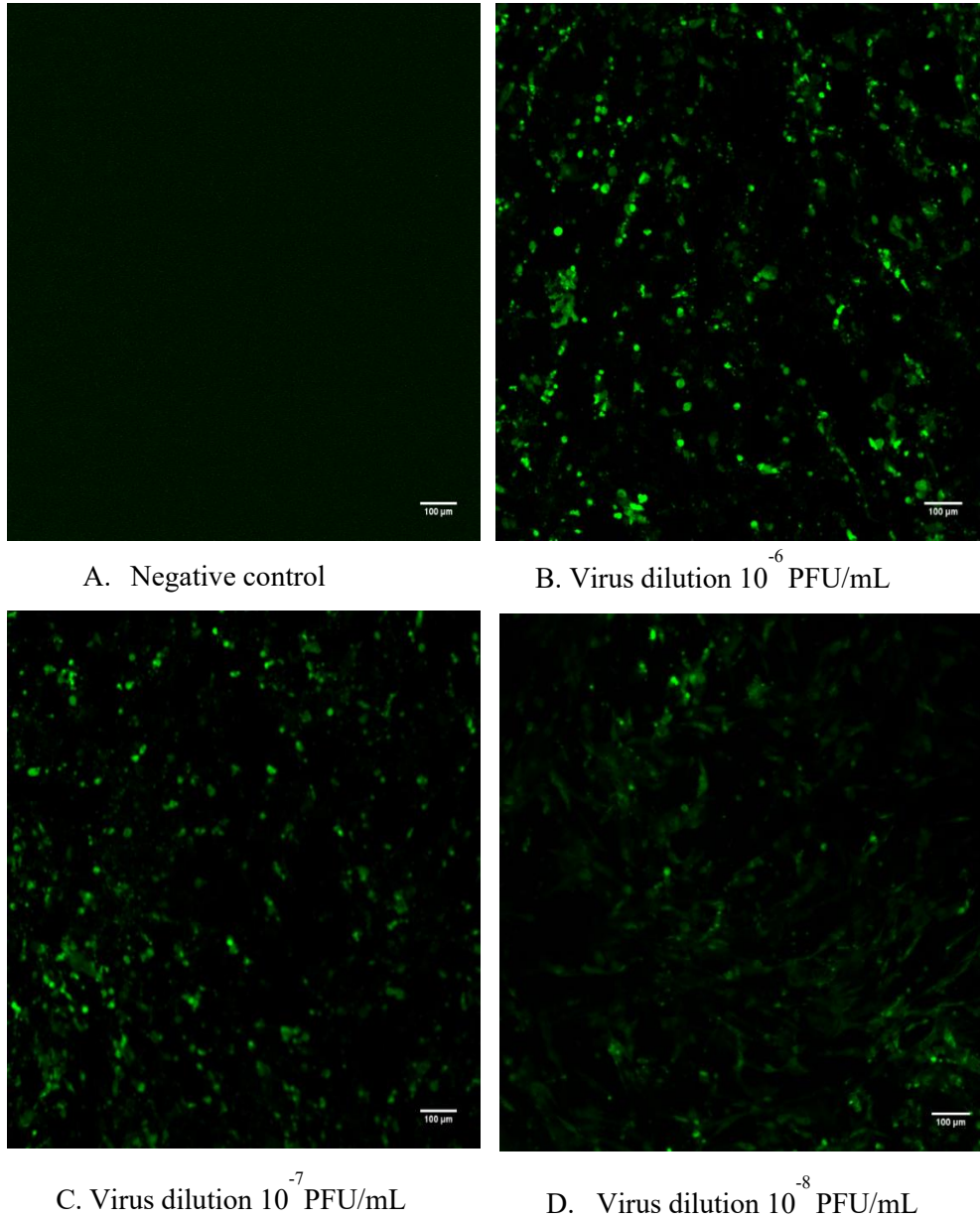


Fig. 4 Plaque assay showing dilutional effect of SINV. Baby hamster kidney-21 cells were infected with SINV-TaV-GFP and the final titer was calculated using plaque counts and known dilution factors.

Distribution of SINV infection foci in Aedes aegypti

Female *Aedes aegypti* mosquitoes were challenged with a viremic bloodmeal at day 5 – 7 post-emergence (p.e.). Midguts were dissected directly into chilled PBS in a glass-bottomed cell culture dish on days 5 and 7 and fixed with 4% paraformaldehyde/PBS solution for 10 min at RT. Guts were thrice rinsed in PBS and visually examined for SINV-associated GFP fluorescence via an Olympus confocal microscope.

Initial infection focus of midgut was localized in cells at the PMG and spread to cells in other areas of the midgut towards the foregut region. Clustered infection foci originating from the initial infection site were observed to include approximately 50% of the midgut epithelia whereas peristaltic muscles did not present GFP fluorescence, suggesting the virus had not yet disseminated from the gut epithelia to secondary tissues at day 5 p.i. (Fig.5).

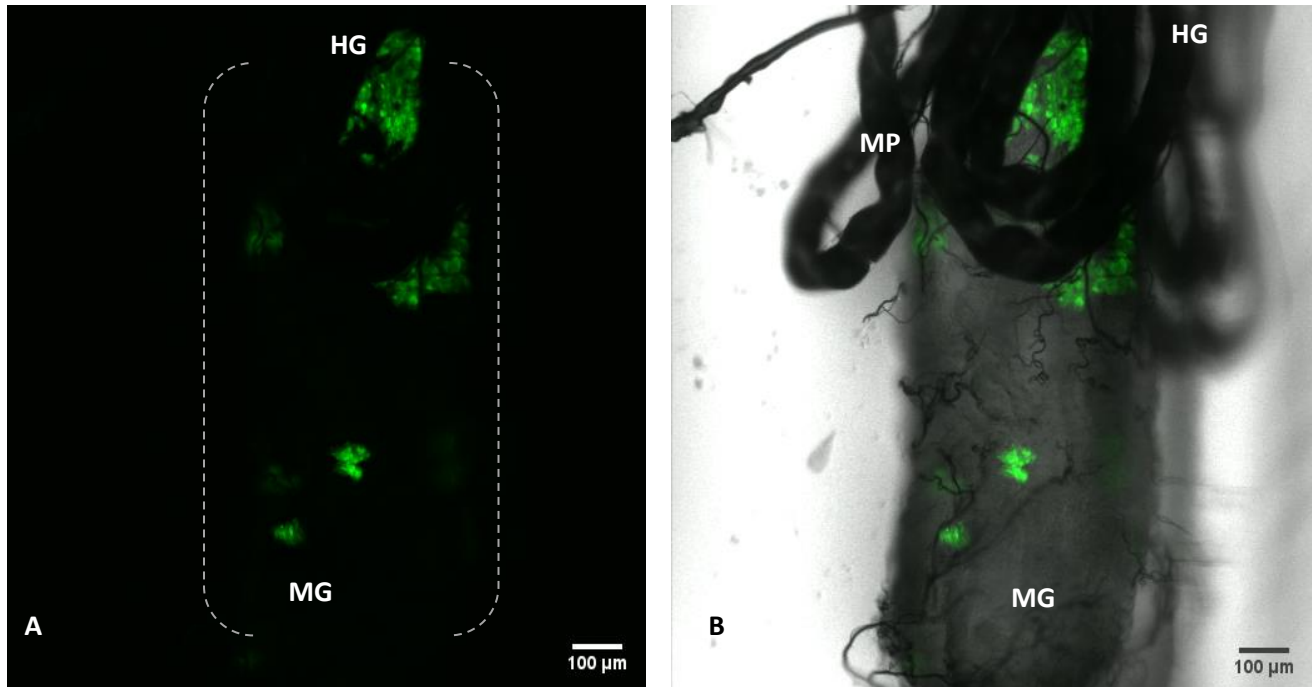


Fig. 5 Laser confocal image (A) and bright field overlay (B) of multiple SINV-TaV-GFP infection foci in the midgut of *Ae. aegypti* on day 5 p.i. Female mosquitoes were proffered viremic bloodmeal and guts were dissected on day 5 p.i. SINV infection foci are shown as green fluorescent clusters. Width of the midgut (white dashes; A). HG: hindgut MP: Malpighian tubules. MG: midgut. 100X.

Distribution of FMRFamide positive ECs

To understand the potential role of ECs in SINV dissemination, the distribution of ECs was investigated within the mosquito posterior midgut where blood digestion occurs. Mosquito midguts were dissected on day 5 p.e. and fixed in chilled 4% paraformaldehyde/PBS overnight. Antibody against FMRFamide was used for the detection of ECs positive for FMRFamide in the mosquito midgut and visualized via a secondary antibody conjugated with TX-red fluorochrome. Spatial distribution of most ECs was observed

in the PMG-m and PMG-c although FMRFamide positive ECs were also observed in the PMG-f (Fig. 6). Previous research indicate that ECs are most abundant in the PMG of female mosquitoes where blood digestion takes place (Brown, 1985) and our data supports this in *Ae. aegypti*.

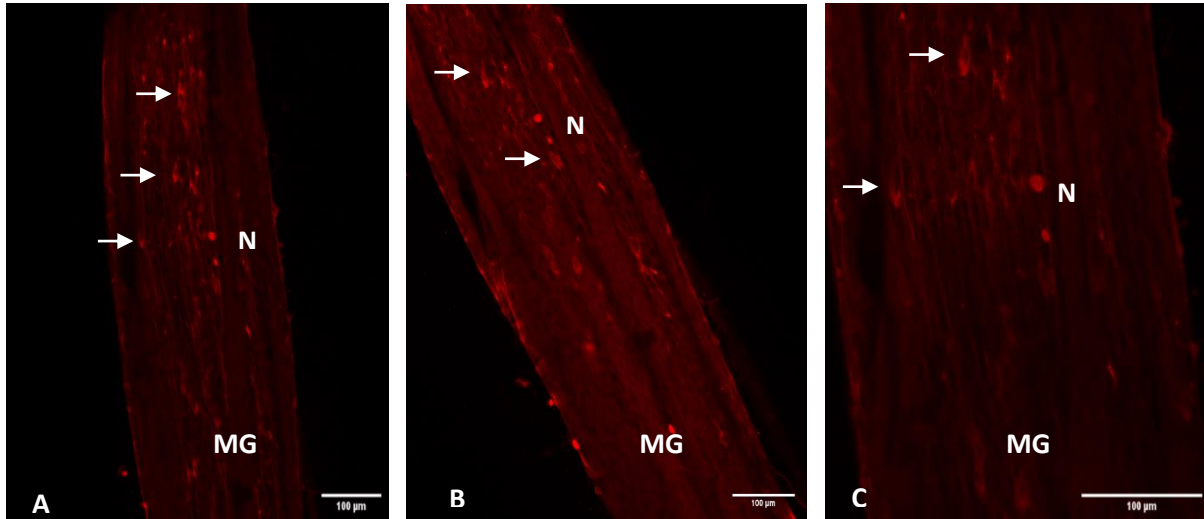


Fig. 6 Distribution of ECs in the mosquito PMG on day 5 p.i. ECs with FMRFamide granules are demonstrated by TX-Red fluorescence and indicated by white arrows in all three images. N: potential neuron. MG: midgut. A. 100X B. 200X. C. 400X

Overlay of GFP infection foci and FMRFamide-positive ECs

In order to decipher the identity of mosquito gut cells with GFP sequestrations, and possibly the role of these cells in virus dissemination from the gut, we first infected female *Ae. aegypti* with SINV-TaV-GFP and followed by identifying ECs positive for FMRFamide. Distribution of ECs was observed along the entire length of the gut as well as some neurons which were also reactive to FMRFamide antibody (Fig. 7). GFP accumulations sequestered in gut cells were evident by day 5 p.i. (Fig 7 B & C) and formed a single infection foci in the epithelia of the PMG-m (Fig. 7 B & C); however, dissemination of virus was not observed due to the absence of infections in the peristaltic muscles in the gut. Figure 7 D showed a merged image of the GFP accumulations in gut cells with FMRFamide-positive ECs where colocalization of the two was not evident. Figure 8 demonstrates an GFP infection foci in the PMG-c region of another female *Ae. aegypti* on day 7 p.i. Scattered FMRFamide-positive ECs were concentrated in the PMG-m and a few

scattered ECs were noted near the GFP infection foci. However, we did not observe colocalization of GFP accumulation and TX-Red labelled ECs. In comparison to day 5 dissected gut, there was an overall reduction in intensity of FMRamide fluorescence and also appeared to be less ECs in the gut on day 7 p.i.

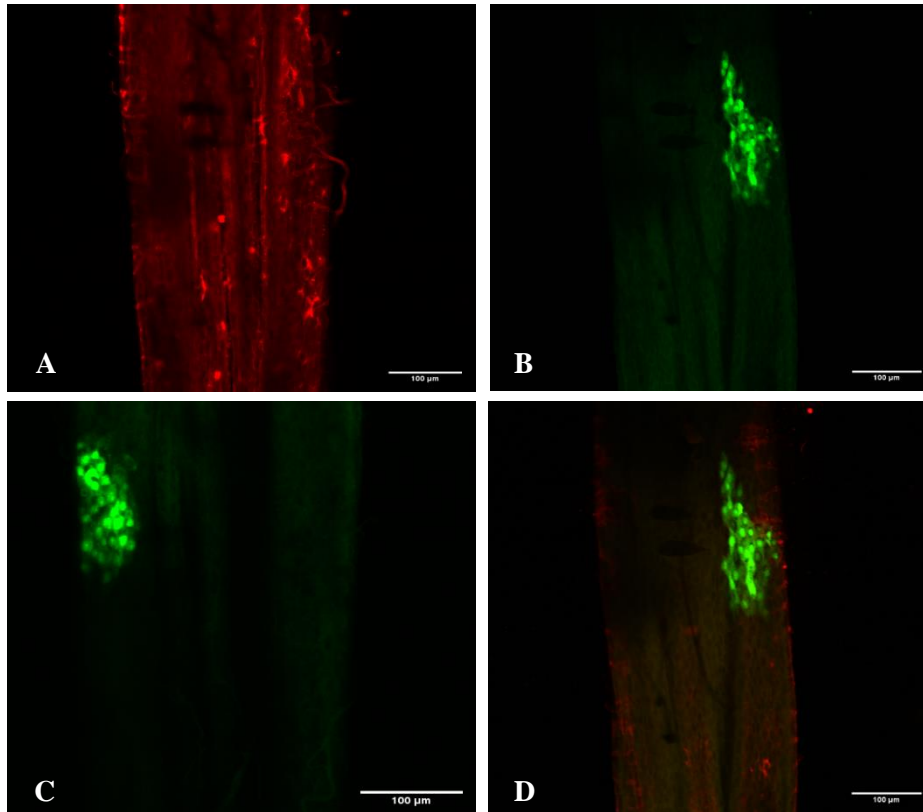


Fig. 7 Confocal fluorescent images of FMRamide positive ECs (A) and a single GFP focus extending from front to back of the midgut (B & C) and overlay of the GFP infection foci and TX-Red fluorescence (D). Midgut of a female *Ae. aegypti* dissected on day 5 p.i. GFP infection foci did not colocalize with FMRamide-positive ECs. 200X.

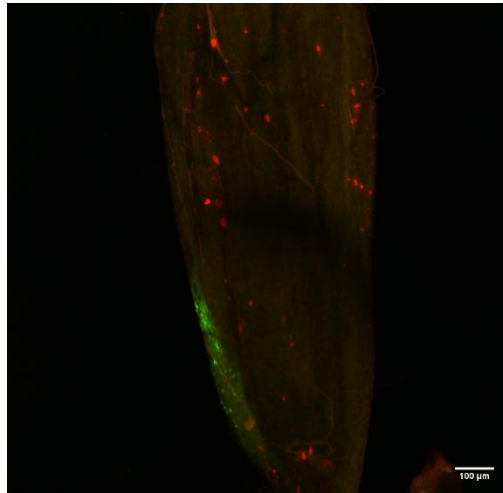


Fig. 8 Overlay confocal fluorescent image of FMRFamide positive ECs and a GFP infection foci in the PMG-c region of a female *Ae. aegypti* dissected on day 7 p.i. with SINV. GFP infection foci did not colocalize with FMRFamide-positive ECs. 200X.

Further experiments examining the distribution of GFP accumulations and FMRFamide, demonstrated colocalization of SINV infection foci and ECs in the midgut of a female mosquito on day 7 p.i. Confocal analysis of the midgut demonstrated GFP accumulations in gut cells forming a single infection foci in the posterior midgut region (Fig. 9 A) and the presence of FMRFamide positive ECs (Fig. 9 B) in the same region. Hindgut was draped over portion of the midgut forming a fold in the middle midgut region. Overlay of the GFP accumulations and FMRFamide positive ECs demonstrated colocalization of the two (shown in yellow; Fig. 9 C), suggesting that ECs were involved in the initial virus infection of the gut epithelia and possibly playing a role in the virus dissemination from the gut. This phenomenon was repeated in additional experiments with mosquito 2 and 3 where concentrations of GFP in the foci and ECs colocalized at distinctive sites in the PMG-c (Fig 10 C & D; Fig 11 D). Dissemination of virus was not observed from GFP presenting cells to peristaltic muscle bundles in the gut shown here. GFP accumulations were visible in mosquito 3 but not in mosquito 1 and 2 as shown below.

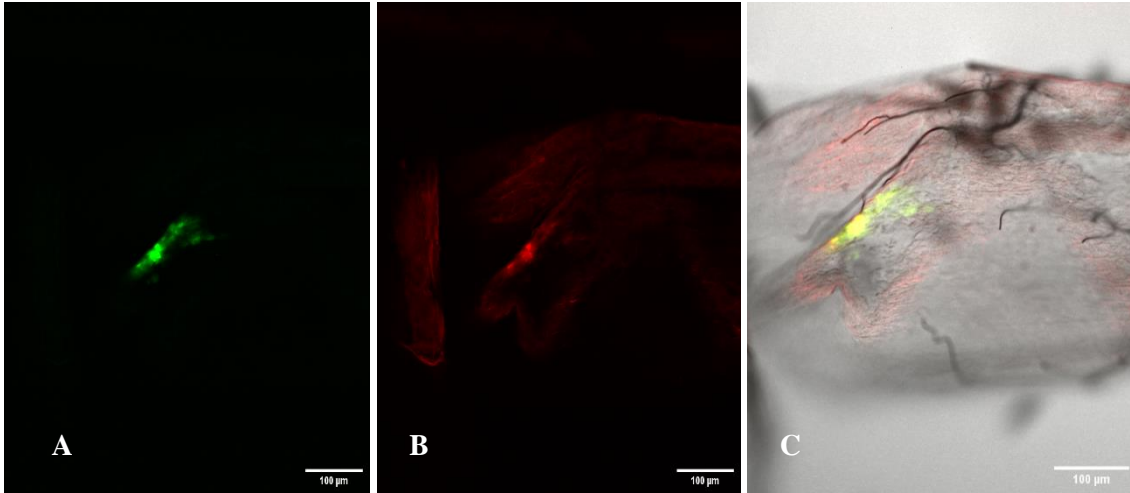


Fig. 9 Comparison of SINV associated GFP (A) and ECs TX-Red (B) in PMG-m infection focus in mosquito-1 at day 7 p.i. A. SINV associated GFP accumulations at the basolateral aspect of the PMG. B. FMRFamide-positive ECs on the basal aspect of the PMG region. A & B 200X. C. Overlay of A&B. 200X.

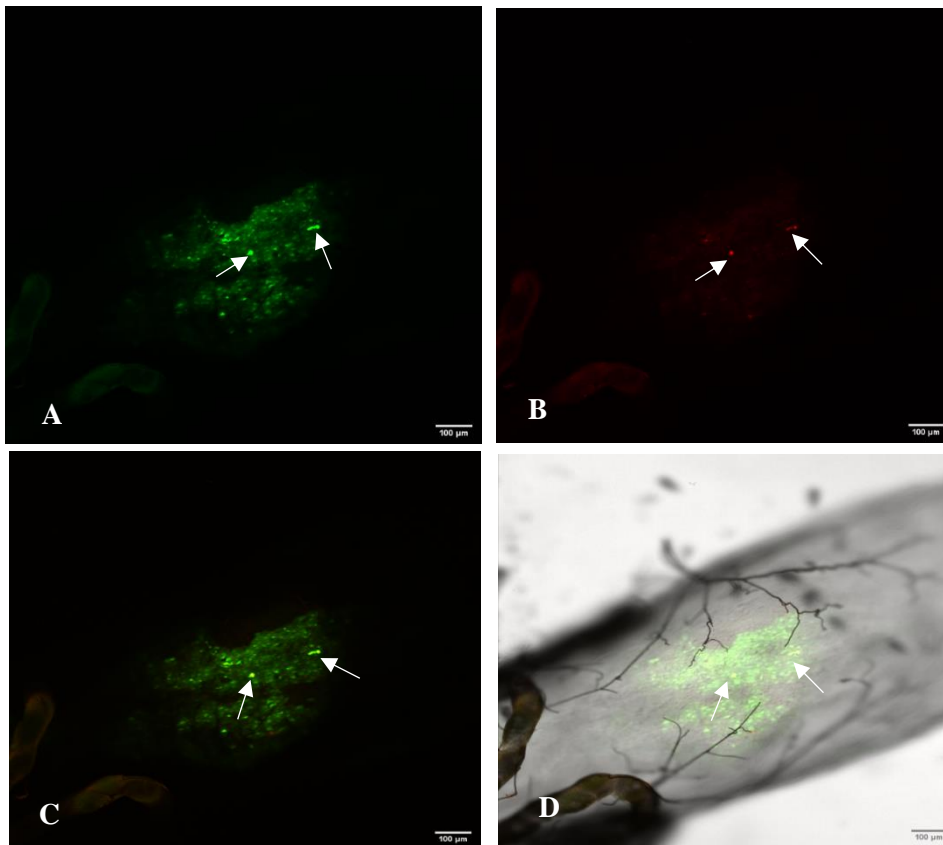


Fig. 10 GFP accumulations and FMRFamide immunoreactivity in PMG of mosquito-2 on day 7 p.i. ECs are indicated with white arrows. A. GFP accumulations, 200X. B. FMRFamide immunoreactive ECs. 200X. C. Overlay of GFP accumulations and ECs at two distinctive sites, 200X. D. DIC image showing the colocalizations, 200X.

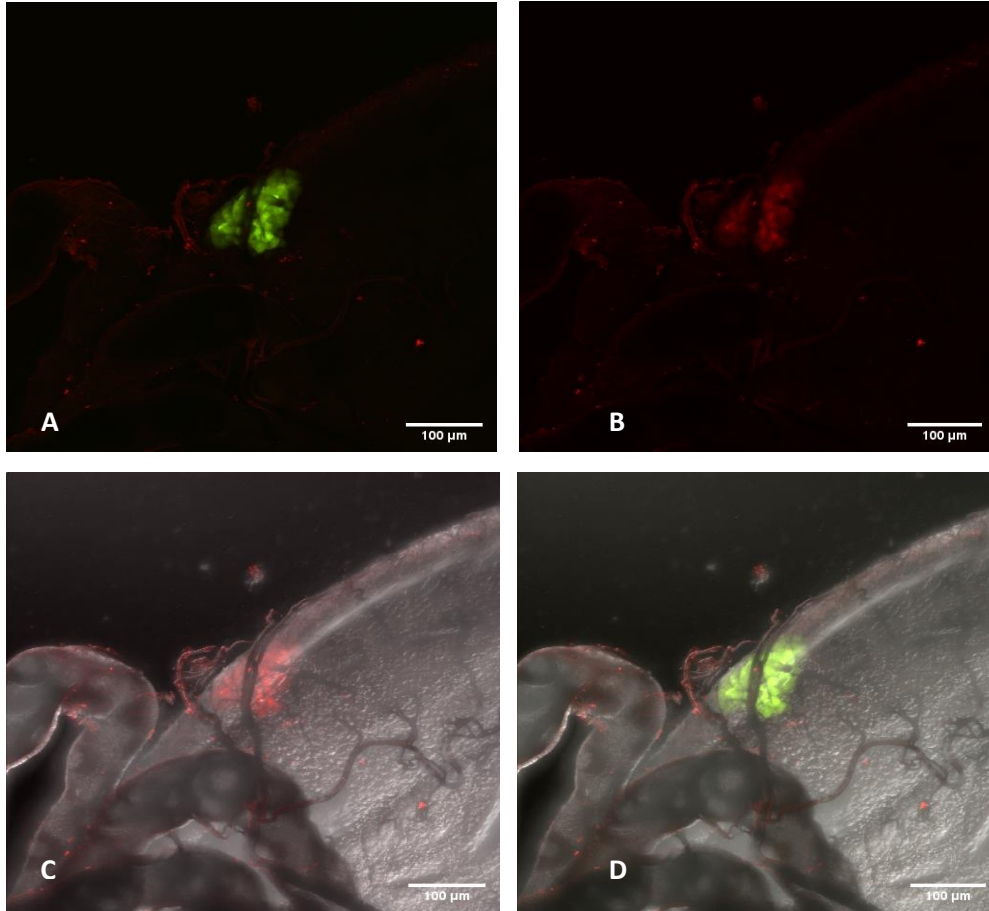


Fig. 11 Confocal analysis of GFP infection foci and ECs in the PMG region of mosquito-3 day 7 p.i. A. Single GFP infection focus. B. FMRamide positive ECs. C. Confocal microscopy with brightfield overlay showing ECs and the structure of the midgut. D. Overlay of A, B, & C showing GFP accumulations in ECs. 200X.

Following a viremic bloodmeal, mosquito guts were dissected at day 7 p.i. for determining the percent of SINV infection and foci distribution via confocal microscopy (Table 1). Presence or absence of SINV associated GFP foci were indicative of permissive (infected) vs refractory (noninfected) mosquitoes. Out of 215 mosquitoes surveyed, 35% of the mosquitoes were permissive to SINV-TaV-GFP making it a moderately infectious arbovirus. It is important to note that majority of SINV-TaV-GFP foci were observed in the PMG-m while the rest of GFP foci were observed in lesser numbers in PMG-f and PMG-c.

Table 1. Percent infection of mosquito midguts and distribution of SINV associated GFP foci in midguts at day 7 p.i.

	Mosquito infected	PMG-f	PMG-m	PMG-c
Trial 1	36/76 = 47%	14/67 = 21%	42/67 = 63%	11/67 = 16%
Trial 2	11/20 = 55%	5/15 = 33%	7/15 = 47%	3/15 = 20%
Trial 3	6/41 = 15%	4/9 = 44%	2/9 = 22%	3/9 = 33%
Trial 4	22/78 = 28%	9/21 = 42%	6/21 = 29%	6/21 = 29%
Total	75/215 = 35%	32/112 = 29%	57/112 = 51%	23/112 = 21%

Distribution of ECs in response to bloodmeal treatments

In order to determine the physiological reasoning behind the overall reduction of FMRFamide positive ECs in the midgut, we examined the distribution of ECs in response to different bloodmeal treatments. Cohorts of female mosquitoes of day 5 p.e. were subjected to non-bloodmeal, regular bloodmeal, viremic bloodmeal treatments for an hour at standard insectary conditions. Mosquito midguts were dissected on days 0, 5, 7 post treatments and FMRFamide distribution were documented via confocal microscopy. Fluorescent signals of ECs were the most evident in non-bloodfed on days 0 (Fig.12) and 5 (Fig.13), followed by viremic bloodfed mosquitoes on days 5 (Fig. 14) and 7 (Fig. 16), whereas the least ECs fluorescence was observed in bloodfed mosquitoes on day 7 (Fig. 15). SINV infection foci were observed in two mosquitoes on days 5 and 7, respectively, but the foci did not coincide with any ECs in the basal aspect of the mosquitoes (Data not shown).

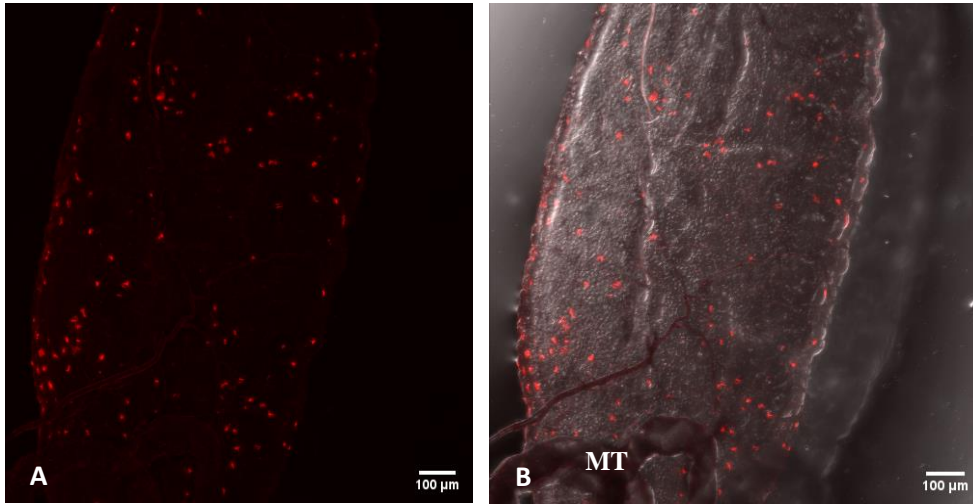


Fig. 12 Confocal microscopy showing distribution of ECs in midgut of a non-bloodfed female mosquito. Immunoreactive ECs are peppered along the entire length of the PMG. A. Confocal microscopic image of ECs. B. Brightfield overlay showing overall structure of the gut. Malpighian tubules (MT) are present to indicate posterior midgut region. 200X.

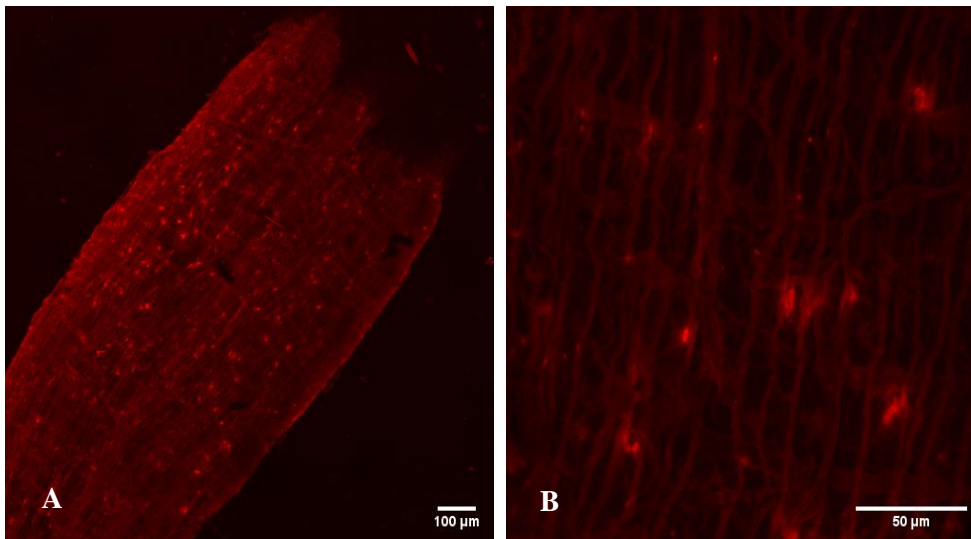


Fig. 13 Confocal microscopy showing distribution of ECs in midgut of a bloodfed female mosquito on day 5 post feeding. Immunoreactive ECs are shown along the entire length of the PMG. A. Confocal microscopic image of ECs. 200X B. Confocal image of the same mosquito showing structure of ECs.600X.

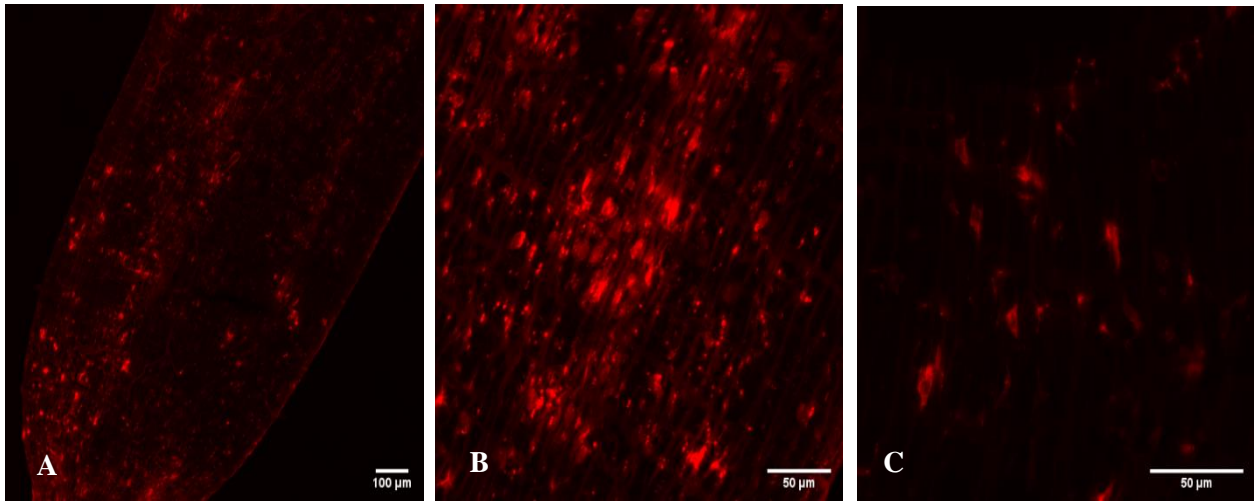


Fig. 14 Confocal microscopy of ECs in PMG at day 5 post viremic bloodfed female mosquito. Immunoreactive ECs are observed along the entire length of the PMG. A. Confocal microscopic image of ECs. 200X B. Confocal image demonstrating structures of ECs and peristaltic muscle bundles. 40X. C. Confocal image showing individual ECs. 600X.

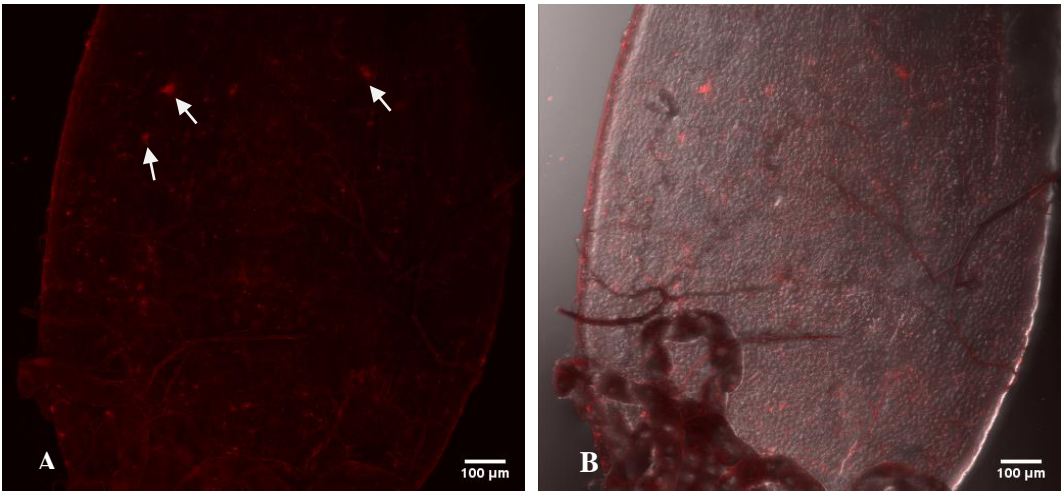


Fig. 15 Confocal microscopy of ECs in PMG at day 7 post bloodfed female mosquito. A few immunoreactive ECs indicated by white arrows were observed in the basal aspect of the midgut. A. Confocal microscopic image of ECs. 200X. B. Confocal image showing the structure of the midgut. 200X.

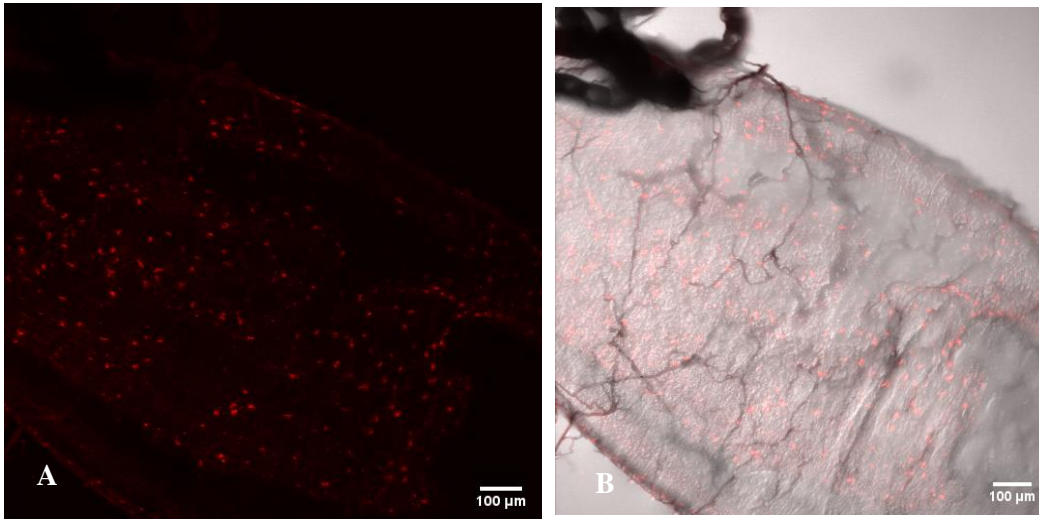


Fig. 16 Confocal microscopy of ECs in midgut of day 7 post viremic bloodfed female mosquito. Immunoreactive ECs were observed in the basal aspect of the PMG. A. Confocal microscopic image of ECs. 200X. B. Confocal image showing the structure of the midgut. 200X.

Table 2 shows the number of mosquitoes positive for FMRFamide following differential bloodmeal treatments on day 5 and 7. Cohorts of mosquitoes were separated into different cages prior to bloodfeeding. At day 0, mosquitoes in the control group did not receive any blood and were placed on a sugar diet while rest of the mosquitoes either received a normal bloodmeal or a viremic bloodmeal. Detection of FMRFamide in gut cells was observed in non-bloodfed mosquitoes at day 0 and mosquitoes received either normal or viremic bloodmeal at day 5 and 7 post feeding. Surprisingly mosquitoes received viremic bloodmeal on both day 5 and 7 had the highest percentage of FMRFamide positive guts compared to the control group. While there was a stark difference in percent FMRFamide positive midguts received a normal bloodmeal day 5 and 7, but there was no difference between viremic bloodfed groups on day 5 and 7 (Fig. 17).

Table 2. FMRFamide labeled ECs in mosquitoes receiving different bloodmeal (BM) treatments on day 5 vs day 7. (NBM: normal bloodmeal; VBM: viremic bloodmeal; N/A: not sampled).

	No BM	Normal BM	Viremic BM
Day 0	8/10 = 80%	N/A	N/A
Day 5	N/A	3/4 = 75%	7/8 = 88%
Day 7	N/A	1/5 = 20%	7/8 = 88%

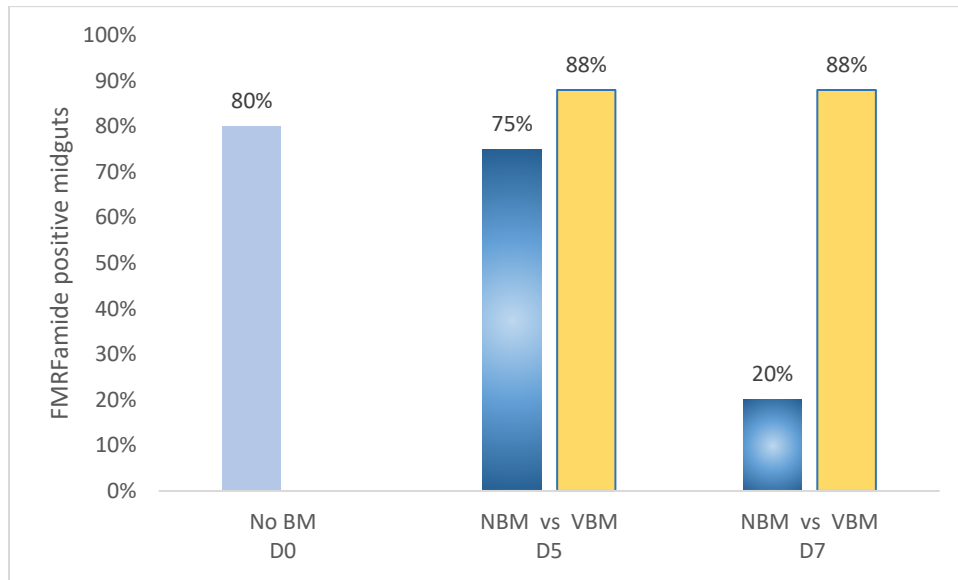


Fig. 17 Comparison of mosquito midguts positive for FMRFamide after bloodfeeding treatments. Female mosquitoes received no bloodmeal (No BM) on day 0, normal bloodmeal (NBM) on day 5 and 7, viremic bloodmeal (VBM) on day 5 and 7.

Persistent SINV infection in Ae. aegypti on day 30

In this study SINV associated GFP foci were first evident at day 5 p.i. and remained persistent until day 7 p.i. Further experiments involving SINV infection in *Ae. aegypti* demonstrated that GFP foci were evident on day 30 p.i. (Fig. 18 A & B) while dissemination of SINV from a single focus to the peristaltic muscle bundles were also observed (Fig. 19). Localized GFP accumulations were first observed in individual cells of the PMG (Fig. 18 A) where Malpighian tubules were evident, and the infection was projected to spread towards cells of the PMG-f portion. Following an oral infection, SINV associated GFP fluorescence was observed in the longitudinal and circular muscles of the PMG-f of a female mosquito at day 30 p.i. This phenomenon indicates dissemination of SINV first from the gut and possibly into the hemolymph and other secondary target tissues. Application of anti-FMRFamide antibody on the infected gut demonstrated presence of ECs scattered in the PMG-f region although GFP fluorescence was not observed in these cells.

Although the GFP was persistent until day 30 p.i., a relatively low infection rate 14% (table 3) was documented compared to that of 35% of day 7 p.i. Furthermore, majority of the GFP foci was located in the PMG-m region while none was observed in PMG-f and one was observed in PMG-c at day 30 p.i.

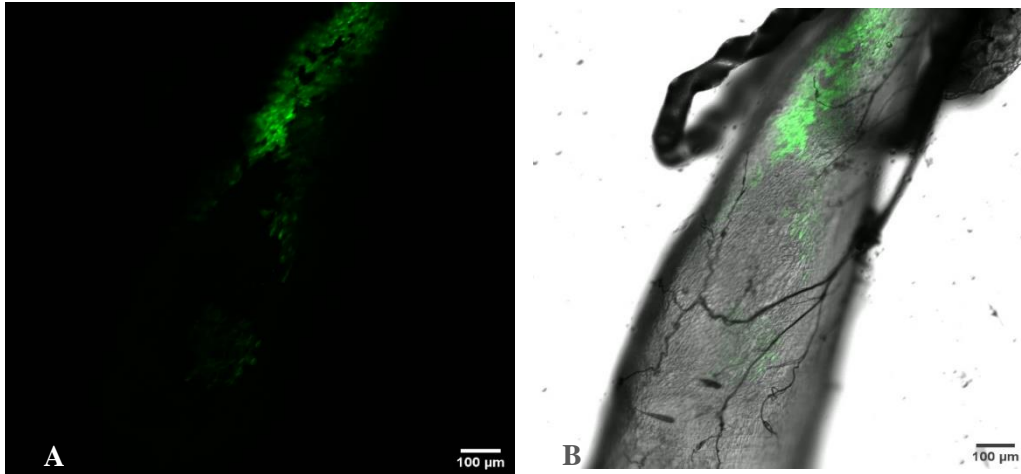


Fig. 18 Confocal microscopy demonstrating a SINV associated GFP foci in the PMG-c of a female mosquito at day 30 p.i. The earliest SINV-TaV-GFP infection was observed on day 3 and persistent infection was observed until day 30 (Saredy et al., 2020; in press). A. SINV associated GFP foci. B. Overlay of bright field microscopy demonstrating site of the infection foci. 10X.

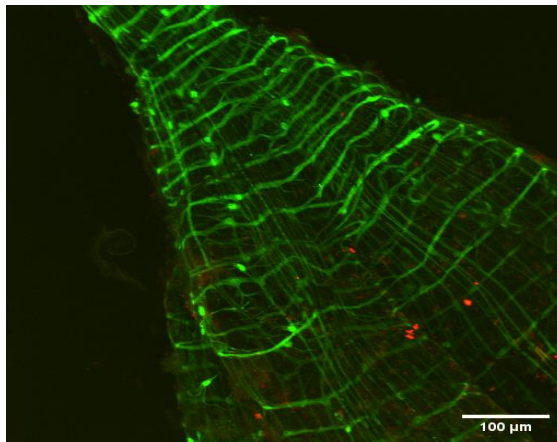


Fig. 19 Confocal microscopy of SINV-TaV-GFP dissemination in the PMG of a female mosquito at day 30 p.i. SINV associated GFP focus is no longer visible at this stage and local dissemination of SINV is confirmed by the infection of the peristaltic muscles in the PMG-f. Anti-FMRamide treatment demonstrates the presence of ECs in red in this region on day 30. 40X.

Table 3. Percent infection and distribution of SINV-TaV-GFP foci in mosquito midgut at day 30 p.i. G Mosquito infected.

Mosquito infected	PMG-f	PMG-m	PMG-c
6/43 = 14%	0	6	1

Multiple infection foci in Ae. aegypti

Multiple infection foci (> 10) were observed in all three segments of the midgut of a female on day 7 p.i. as shown in Fig. 20. This finding presents an outlier from all other mosquitoes utilized in this experiment, which may represent physiological differences in individuals. It is also interesting to note that even though SINV was able to infect gut cells in all three distinct regions, the virus was not observed to have disseminated from any infection foci to the muscle bundles.

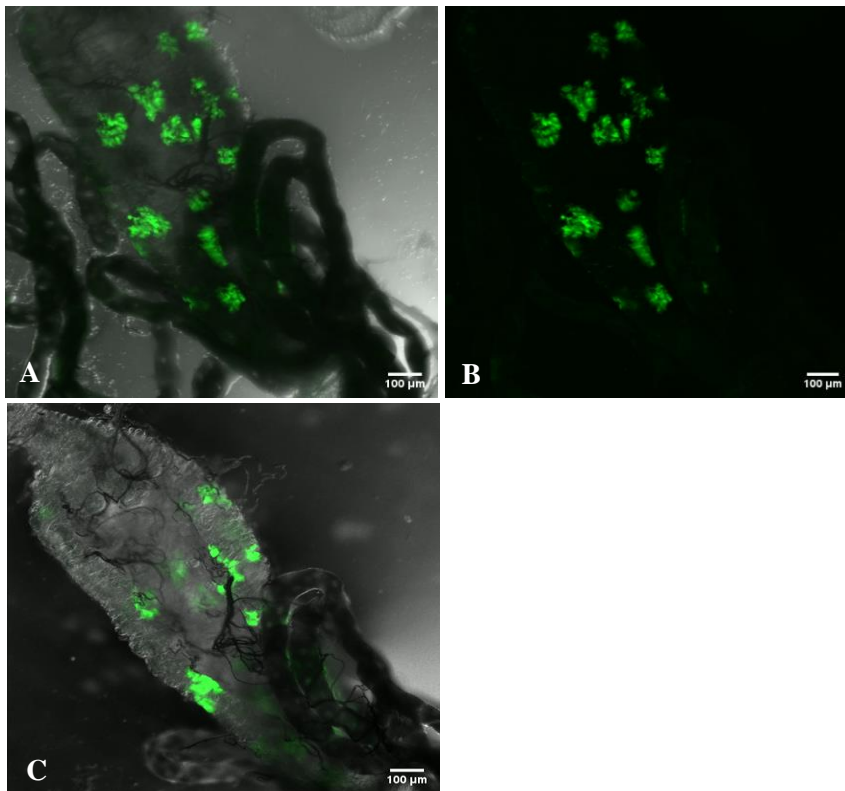


Fig. 20 Multiple GFP foci in PMG region of female mosquito D7 p.i. Female mosquitoes were proffered viremic bloodmeal and midguts were dissected on D7. GFP foci are indicative of the virus infection within the mosquito midgut. 20X.

IV. Discussion

This goal of this study was to investigate the potential roles of ECs in SINV infection and dissemination from the female midgut to other secondary tissues following oral blood feeding. Here we demonstrated that SINV-TaV-GFP was able to infect and multiply in great quantity in BHK-21 cells. Infected BHK-21 cells demonstrated intense SINV associated GFP fluorescence, presented by rounding of the cells which eventually forms a clearing around healthy cells, or virus plaques (Fig. 4 B, C, & D), whereas non-infected BHK cells lacked fluorescence altogether (Fig. 4 A). Virus plaques were then visualized by staining the cells with a neutral red dye that is only taken up by healthy, living cells. Using this cell-based virus plaque assay, we were able to observe the dilutional effects of the virus in cell culture flasks, and more importantly, this enabled us to use the plaque counts to accurately calculate virus titer which was essential in following experiments in this study.

Using the GFP-reporter virus enabled us to map the temporal-spatial timeline of infection and dissemination of gut cells from the mosquito midgut. SINV infection foci were ubiquitously expressed in all three distinct regions of the PMG on both days 5 and 7 p.i. and remained persistent until day 30 p.i., consistent with previous studies (Sareddy et al., 2020). Infection of the PMG cells were first detected on day 5 p.i. in this study although Sareddy and colleagues (2020) demonstrated that SINV infection occurred as early as day 3 p.i. SINV dissemination in peristaltic muscles was detected on day 30 p.i., but not detected on neither day 5 nor day 7 p.i. in this study. A previous study utilizing leg assays indicated that SINV dissemination can occur as early as day 5 p.i. following a viremic bloodfeeding (Sareddy et al., 2020). This difference could be attributed to the sample size of the current study as well as individual physiological differences in mosquitoes. Further experiments demonstrated that SINV has a moderate percent infection in the mosquito PMG with the highest number of GFP infection foci localized in the PMG-m whereas the lesser numbers of GFP foci were identified in the other two regions of the PMG (Table 1) in accordance with previous research by Sareddy and et al. (2020). Interestingly, we discovered a female mosquito midgut infected with SINV displaying multiple GFP foci (>10) at day 7 p.i., which is a highly unusual finding

considering the greatest number of GFP foci documented was three from our previous studies. This, too, demonstrates that individual differences are significant in each mosquito and need to be considered when conducting experiments.

Immunopositive ECs and GFP foci were colocalized at distinct sites in the PMG on day 7 p.i. (Figs. 9, 10 & 11), suggesting involvement of the ECs in SINV infection and possibly dissemination. Upon bloodmeal ingestion, FMRFamide is released from the basolateral aspect of the gut into the hemolymph, where it acts as a paracrine signal to transduce downstream signaling to nearby and distant tissues (Brown et al., 1986). Brown and colleagues (1986) suggest that stretching of the gut due to the presence of bloodmeal may have aided in the release of FMRFamide. Given its cardioexcitatory and myotropic nature, FMRFamide could then stimulate the contraction of the gut peristaltic muscles to move digested bolus bloodmeal past the PMG to the hindgut for excretion (Brown and Lea, 1989). Additionally, FMRFamide could also function as a hormone that diffuses to neighboring digestive cells to stimulate the release of an appropriate amount of digestive enzymes to prevent self-digestion (Brown et al., 1986). Interestingly, relevant sensory cues control secretions of FMRFamide-related neuropeptides in nematodes, where they act directly on the egg-laying motor neurons, thereby directly modulating their reproductive behaviors such as egg-laying and copulation (Waggoner et al., 2000; Kim and Li, 2004; Ringstad et al., 2008). Given the abundance and physiological complexity of ECs, we suggest that SINV uses ECs as the gateway to initiate infection and subsequently hijack the unique secretory function of the cells for its dissemination from the midgut epithelia.

Following bloodmeal treatments, non-bloodfed mosquitoes appeared to exhibit the most abundant FMRFamide positive cells in the midgut (Fig. 12), followed by normal bloodfed group (Fig. 13), and virus bloodfed groups at days 5 (Fig. 14) and 7 (Fig. 16). The least abundant of FMRFamide positive ECs were observed in Day 7 normal bloodfed group (Fig. 15). These findings suggest that FMRFamide is retained in the midgut ECs of both non-bloodfed and viremic bloodfed mosquitoes on days 5 and 7 p.i. There was no overall reduction in the intensity of FMRFamide fluorescence or the abundance of ECs for viremic bloodfed groups. Majority of the granules were released on day 7 following a normal bloodmeal, and there was an

overall reduction the FMRFamide fluorescence as well as the number of immunoreactive ECs. Brown and Lea (1989) reported that ingestion of bloodmeal reduces the number of immunoreactive cells by half in the mosquito PMG, thereby suggesting that bloodfeeding either promotes the release of the neuropeptide from ECs or decreases its synthesis. It has also been speculated that secretions from ECs may contain factors that aid oocyte production and maturation for female mosquitoes (Brown et al., 1986). Our data with normal bloodfed group supports Brown's findings, however, the observations for the viremic bloodfed groups contradicted Brown's results. Furthermore, in a study involving fed vs starved corn earworm, Jenkins and colleagues (1989) discovered that twice as many of FMRFamide immunoreactive cells and four times as many of FMRFamide neuropeptides are found in the midguts of fed earworms in comparison to starved earworms. At first glance, these contradicting observations cannot form a consistent pattern to help decipher our results from the bloodfeeding treatments. However, a study by Zitana and colleagues (1995) found that parasitism by wasps in *Manduca sexta* larvae induces accumulation of FMRFamide in the ECs, which could be triggered by polydnavirus injection by wasp into the host upon contact. They suggest that this phenomenon can be caused by either suppression of the peptide release or elevation in the rate of peptide synthesis as an immune response by parasitized larvae. Therefore, we speculate that SINV infection could also contribute to the accumulations of FMRFamide in the ECs in the mosquito PMG at days 5 and 7 p.i. Furthermore, it is worth noting that some neural processes were also immunoreactive to FMRFamide antibody (Fig. 6).

This study demonstrated a novel finding that SINV could initiate infection in ECs and potentially utilizes the neurosecretory nature of the ECs to disseminate to neighboring gut cells and distant target tissues. Our findings contributed to the current understanding of the underlying mechanism that arboviruses utilize to overcome infection and dissemination barriers in their vectors. However, our study does not negate other potential avenues arboviruses could exploit for establishing successful and persistent infection in their hosts. Further studies are needed to determine whether viremic bloodfeeding could indeed lead to the accumulation of FMRFamide in mosquito ECs in contrast to normal bloodfeeding. Furthermore, we need to investigate which biochemical pathways are triggered in regard to the accumulation or release of

FMRamide during bloodfeeding. Due to global warming, disease-carrying vectors will spread to areas where arbovirus outbreaks are not typically a concern, it is crucial for us to gain more understanding of arbovirus transmission and host response to infection to combat future infectious disease outbreaks.

References

- Bar-Zeev, M. 1958. The effect of temperature on the growth rate and survival of the immature stages of *Aedes aegypti* (L.). *Bull. Entomol. Res.* 49: 157–163.
- Bowers, D.F., Abell, B.A., Brown, D.T. 1995. Replication and Tissue Tropism of the Alphavirus Sindbis in the Mosquito *Aedes albopictus*.
- Brown, M. R., Raikhel, A. S., & Lea, A. O. (1985). Ultrastructure of midgut endocrine cells in the adult mosquito, *Aedes aegypti*. *Tissue and Cell*, 17(5), 709-721.
- Brown MR, Crim JW, Lea AO. 1986. FMRFamide and pancreatic polypeptide-like immunoreactivity of endocrine cells in the midgut of a mosquito. *Tissue and Cell* 18: 419-428.
- Byrnes A, Griffin D. 1998. Binding of Sindbis virus to cell surface heparan sulfate. *Journal of Virology*. 72 (9):7349-7356
- Clements A.N. 1996. The Biology of Mosquitoes; Chapter 13 Structure of the adult alimentary canal. Chapman and Hall London. pp.263-271.
- Dockary, G.J., Vaillant, C. and Williams, R.G. 1981. New vertebrate brain-gut peptide related to a molluscan neuropeptide and an opioid peptide. *Nature*, London., 293, 656-657.
- Greenberg, M.J. and Price, D.A. 1983. Invertebrate neuropeptides: native and naturalized. *Annual Review of Physiology*, 45, 271-288.
- Hales, S., P. Weinstein, Y, Souras. 1999. El Nino and the dynamics of vector borne disease transmission. *Environmental Health Prospect*. 107:99-102
- Hardy, J.L., Houk, E.J., Kramer, L.D., Reeves, W.C. 1983. Intrinsic factors affecting vector competence of mosquitoes for arboviruses. *Annual Review Entomology*. 28, 229-262.
- Jose J., Snyder J.E., Kuhn R.J. 2009. A structural and functional perspective of alphavirus replication and assembly. *Future Microbiology*; 4: 837–856. DOI: <http://dx.doi.org/10.2217/fmb.09.59>.
- Kim K., Li C. 2004. Expression and regulation of an FMRFamide-related neuropeptide gene family in *Caenorhabditis elegans*. *J Comp Neurol*.475:540–50. doi:10.1002/cne.20189
- Lyski Z, Saredy J, Ciano K, Stem J, Bowers D. 2011. Blood feeding position increases success of recalcitrant mosquitoes. *Vector-borne and Zoonotic Diseases*. 11(8): 1165-1171.
- Lyski, Z.L. 2013. Arbovirus persistence and selection of persistent variants following chronic infection in Aedine mosquitoes: a comparative study between *Ae. aegypti* and *Ae. albopictus* 30 days post infection with Sindbis virus. UNF Thesis and Dissertations. 430.

- Okuda, K., F. de Almeida, R.A. Mortara, H. Kriegar, O. Marinotti, and A.T. Bijovsky. 2007. Cell death and regeneration in the midgut of the mosquito, *Culex quinquefasciatus*. *Journal of Insect Physiology*. 53:1307-1315.
- Parikah, GR, Oliver, JD, Batholomay, L.C. 2009. A Haemocyte tropism for an arbovirus. *Journal of General Virology*. 90: 292-296.
- Ringstad N., Horvitz H.R. 2008. FMRFamide neuropeptides and acetylcholine synergistically inhibit egg-laying by *C. elegans*. *Nat Neurosci*.11:1168–76. doi:10.1038/nn.2186
- Rose, P.P.; Hanna, S.L.; Spiridigliozzi, A.; Wannissorn, N.; Beiting, D.P.; Ross, S.R.; Hardy, R.W.; Bambina, S.A.; Heise, M.T.; Cherry, S. 2011. Natural resistance-associated macrophage protein is a cellular receptor for Sindbis virus in both insect and mammalian hosts. *Cell Host Microbe*.10, 97–104.
- Saredy, J.J. 2015. Infection and Dissemination of TaV-GFP Tagged Sindbis in Aedine Mosquitoes and Cell Lines. UNF Graduate Theses and Dissertations. 554. <https://digitalcommons.unf.edu/etd/554>
- Saredy, J., Chim, F., Lyski, Z., Ahearn, Y., & Bowers, D. (n.d.). Confocal Analysis of the Distribution and Persistence of Sindbis Virus (TaV-GFP) Infection in Midguts of *Aedes aegypti* mosquitoes. *Microscopy and Microanalysis*, 1-8. doi:10.1017/S1431927620001270
- Sperança M.A., Martins Ribolla P.E., Capurro M.L. 2006. Transgenic Vectors: Anopheles and Aedes. Bethesda (MD): National Center for Biotechnology Information (US); 2008. Chapter B04.
- Spuul P., Balistreri G., Hellstrom K., et al. 2011. Assembly of alphavirus replication complexes from RNA and protein components in a novel trans-replication system in mammalian cells. *Journal of Virology*. 85: 4739–4751. DOI: <http://dx.doi.org/10.1128/JVI.00085-11>.
- Strauss E.G., Rice C.M., Strauss J.H. 1984. Complete nucleotide sequence of the genomic RNA of Sindbis virus. *Virology*. 133: 92–110. DOI: [http://dx.doi.org/10.1016/0042-6822\(84\)90428-8](http://dx.doi.org/10.1016/0042-6822(84)90428-8).
- Strauss J.H., Strauss E.G. 1994. The alphaviruses: gene expression, replication, and evolution. *Microbiological Reviews*; 58: 491–562.
- Sun C., Gardner C.L., Watson A.M., Ryman K.D., Klimstra W.B. 2014. Stable, high-level expression of reporter proteins from improved Alphavirus expression vectors to track replication and dissemination during encephalitis and arthritogenic disease. *Journal of Virology*. 88(23): 2035- 2046
- Taylor, R.M., T.H. Hurlbut, J.R. Work, J.R. Kingston, and T.E. Frothingham. 1955. Sindbis virus: newly recognized arthropod transmitted virus. *Am. J. Trop. Med. Hyg*. 4:844-862.
- Turunen M., Kuusisto P., Uggeldahl P.E., Toivanen A. 1998. Pogosta disease: clinical observations during an outbreak in the province of North Karelia, Finland. *Br J Rheumatol*. 37(11):1177-80. PubMed PMID: 9851265.

- Vancini R, Wang G, Ferreira D, Hernandez R, Brown DT. 2013. Alphavirus genome delivery occurs directly at the plasma membrane in a time- and temperature-dependent process. *Journal of Virology*. 87: 4352-4359.
- Veenstra, J.A., Lau, G.W., Agricola, H.J., Petzel, D.H. 1995. Immunobiological localization of regulatory peptides in the midgut of the female mosquito *Aedes aegypti*. *Histochemie*. DOI:10.1007/BF01458127.
- Veenstra, JA. 1999. Isolation and identification of three RFamide immunoreactive peptides from the mosquito *Aedes aegypti*. *Peptides*. 18:937-942.
- Waggoner LE, Hardaker LA, Golik S, Schafer WR. 2000. Effect of a neuropeptide gene on behavioral states in *Caenorhabditis elegans* egg-laying. *Genetics* **154**:1181–92.
- Walsh, J. H. 1981. Gastrointestinal hormones and peptides. In *Physiology of the Gastrointestinal Tract*. Vol 1, pp.59-144. Raven Press. New York.
- WHO. 2017. World malaria report. World Health Organization, Geneva.
- WHO. 2018. Climate change and health. World Health Organization, Geneva.
- WHO. 2020. Vector-borne diseases. World Health Organization, Geneva.
- Zitana D., Kingan T.G., Beckage N.E. 1995. Parasitism induced accumulation of FMRFamide-like peptides in the gut innervation and endocrine cells of *Manduca sexta*. *Insect Biochem. Molec. Biol.* 25: 669-678.

Vita

Yani Pan Ahearn

Born

Re 1993
da
cte
d

Redacted China

EDUCATION

Master of Science in Biology

University of North Florida

Jacksonville, FL

May 2020

Bachelor of Science in Biology

University of North Florida

Jacksonville, FL

August 2017

RESEARCH

Graduate Research Assistant – Dr. Bowers, Professor of Biology

August 2017 – Present

University of North Florida

Jacksonville, FL

EMPLOYMENT

Graduate Teaching Assistant – GBI Lab Instructor

January 2018 – August 2019

University of North Florida

Jacksonville, FL

Medical Technologist II

September 2019 – Present

Florida Department of Health

Jacksonville, FL

CONFERENCE PRESENTATION

Yani P. Ahearn, Jane Benoit, Jason I. Saredy, David Waddell, Doria F. Bowers.

“Sindbis Virus Infects Specific Cells in the Mosquito Posterior Midgut”. Poster presentation”. American Society for Virology annual conference. Minneapolis, Minnesota, USA, 2019.